Influence of band shift induced by different Al content on optoelectronic properties of AlGaN materials

DAOHUA WU[1,2], SHIJIN ZHONG[1,2], MINGJUN HAN[1,2], GUANGZHEN DAI[1,*]
[1]*Anhui Engineering Research Center of Vehicle Display Integrated Systems, School of Integrated Circuits, Anhui Polytechnic University, Wuhu 241000, China*
[2]*Joint Discipline Key Laboratory of Touch Display Materials and Devices in Anhui Province, Wuhu 241000, China*

Numerical calculations based on first-principles were applied to study the influence of band shift induced by different Al content on optoelectronic properties of wurtzite $Al_xGa_{1-x}N$ materials. In this study, we construct the $Al_xGa_{1-x}N$ structure by substitutional doping, where one Al atom replaces one Ga atom at different positions within the GaN structure. The results show that the doping of Al content makes the conduction band bottom of $Al_xGa_{1-x}N$ band offset and little changes for the valence band top, which results in significant changing on optoelectronic properties of $Al_xGa_{1-x}N$. It is helpful to finding a new way to improve the light extraction efficiency, and providing more valuable information for materials and devices based on AlGaN.

(Received March 22, 2024; accepted October 2, 2024)

Keywords: GaN-based materials, First-principles, Optoelectronics properties

1. Introduction

As one of the most important III-nitride semiconductor materials, Gallium nitride (GaN), including its ternary alloys $Al_xGa_{1-x}N$, has been widely used in producing light-emitting diodes (LEDs), lasers diodes (LDs), photon detectors, and other photoelectric devices [1]. It has been proved that $Al_xGa_{1-x}N$ energy band gap continuously can be tuned from 1.9 eV to 6.2 eV by controlling the Al content in the alloy [2], which covers wavelengths from the whole visible to deep ultraviolet (UV) spectral range. Up to now, there are lots of theoretical and experimental investigations of electronic and optical properties of GaN, AlN and $Al_xGa_{1-x}N$ [3-11]. In 1907, Fichter synthesized AlN compound for the first time [3], which opened the research prologue in nitride compounds. In 1932, Johnson firstly produced GaN powder by the reaction of NH_3 and Ga at high temperature [4]. However, due to backwardness in material preparing technology, it was difficult to obtain high-quality single-crystal nitride for more information about their physical properties. Until the advent of epitaxial growth technique, especially the breakthrough in metal-organic chemical vapor deposition technology [5], the study of nitrides re-attracted researchers' attention [6-11]. For example, Akasaki et al prepared a high crystal quality GaN using low temperature buffer technique [6] and found that P-GaN materials exhibit good hole conductivity by low energy electron beam irradiation [7]. Brunner prepared $Al_xGa_{1-x}N$ films by plasma induced molecular beam epitaxy, where the molar fraction x of Al content was varied from 0 to 1 [8]. The energy band gap of $Al_xGa_{1-x}N$ was tuned between 3.42 eV and 6.13 eV by changing the molar fraction x. Simultaneously, with the development of computer science, theoretical calculations have become one of the indispensable methods in physical properties of semiconductor materials. First-principles is one of the powerful tools to model materials and predict physical properties of materials [12,13], which has been widely used in studying physical properties of AlGaN material [14-17]. Based on first-principles, Stampfl and Dridi found that an increase in the acceptor ionization energy and the pressure coefficient with increasing x of $Al_xGa_{1-x}N$ [14,15]. Recently, Lu analyzed the influence of lattice structure changes on optical properties of $Al_xGa_{1-x}N$ alloys based on first-principles [16]. In spite of these calculations, the influence of band shift has seldom been investigated even for the wurtzite $Al_xGa_{1-x}N$ structure. For $Al_xGa_{1-x}N$ alloy, the energy band structure is completely different from GaN, especially, the change of molar fraction x of Al content results in the conduction band offset which affects electronic transition and internal quantum efficiency of $Al_xGa_{1-x}N$ materials directly. On the other hand, the extraction efficiency of emitter based on $Al_xGa_{1-x}N$ materials is relatively lower than that based on other semiconductor materials. Therefore, it is important to investigate the influence of band shift on optoelectronic properties of $Al_xGa_{1-x}N$ materials, which is helpful to finding a new way to improve the extraction efficiency, and providing more valuable information for materials and devices based on $Al_xGa_{1-x}N$.

In this paper, we report the influence of band shift, which is induced by changing Al content, on electronic and optical properties of $Al_xGa_{1-x}N$ alloys using the first

principles based on the density functional theory (DFT) and generalized gradient approximation (GGA) functional theory [18,19]. The optoelectronics properties of wurtzite $Al_xGa_{1-x}N$, including band offset, density of state, refractive index, absorption, reflectivity coefficient and energy loss function, are calculated using VASP software package [20]. It provides forth valuable information about influence of band offset on electronic band structure and optical properties of $Al_xGa_{1-x}N$ which is beneficial to improving the light extraction efficiency of $Al_xGa_{1-x}N$ materials.

2. Model and method for calculation

$Al_xGa_{1-x}N$ models are obtained by substitutional doping some Ga atoms with Al atoms based on wurtzite structure GaN crystal which belongs to the P63mc (186) space group. The lattice constants of GaN are described as a=b=3.1972 Å, c=5.2070 Å, c/a=1.628, α=90°, β=90°, and γ =120° before optimization. The GaN supercell model contains 24 Ga atoms and 24 N atoms, the $Al_xGa_{1-x}N$ supercell model is constructed by substitutional doping Ga atom with Al atom at different positions in GaN structure, the molar fraction x of $Al_xGa_{1-x}N$ are selected as 0, 0.2, 0.4, 0.6, 0.8, 1, respectively. The wurtzite $Al_xGa_{1-x}N$ structures are shown in Fig. 1 where the blue, pink and brown balls represent N, Al and Ga atoms, respectively. The $Al_xGa_{1-x}N$ structure is optimized for calculation when Al content changes in the supercell to obtain optimal results.

The calculations are performed using VASP software package based on DFT and GGA functional theory. The interaction between electrons is described using the projected additive waves (PAW) method. After many times convergence tests, the Ga 3d electrons are set as core states, the cutoff energy of plane-wave basis set is set to 450 eV. Before starting calculations, the bulk GaN crystal structure is optimized via a conjugate gradient method by full relaxation. The electron relaxation accuracy is set to 0.001 eV, and the convergence criterion is that the force acting on each atom is less than 0.005 eV/atom. The K-point sampling in the Brillouin integration zones uses the Gamma centered Monkhorst-Pack scheme [21], and the K-point grid is set to 10×10×10.

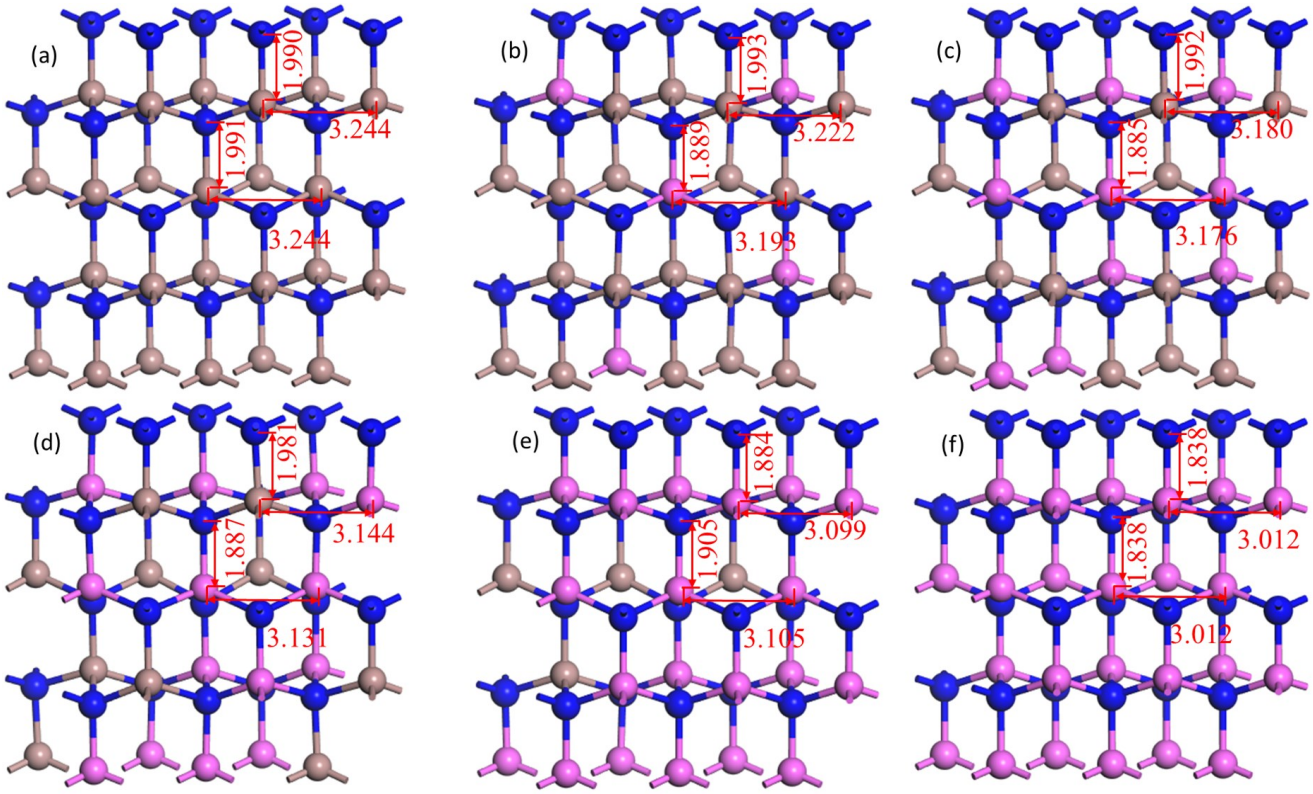

Fig 1. Computational models of (a) GaN, (b) $Al_{0.2}Ga_{0.8}N$, (c)$Al_{0.4}Ga_{0.6}N$, (d) $Al_{0.6}Ga_{0.4}N$, (e) $Al_{0.8}Ga_{0.2}N$ and (f) AlN (color online)

3. Results and discussion

In this section, we will discuss the changes in electronic and optical properties of wurtzite $Al_xGa_{1-x}N$, including energy band structure, density of states, refractive index, absorption coefficient, reflection coefficient and energy loss.

3.1. Energy band structure and density of states of GaN with different Al content

The energy band structure of a semiconductor material determines their characteristics, including electronic and optical properties. The energy band structures of $Al_xGa_{1-x}N$

super cell with different Al content are computed by using GGA approximation which are shown in Fig. 2.

As shown in Fig. 2, the conduction band bottom and valance band top occur at same symmetry point, which indicates wurtzite $Al_xGa_{1-x}N$ possess direct band gap. We can note that the energy band gap of GaN is approximately 1.93 eV, which is slightly lower than that with experimental result. It is due to neglecting the influence of electrons in calculations and can be corrected by adding a scissors since it changes the energy band gap, whereas does not change the conduction band or valence band structure. Thus, it does not affect the analysis of the conduction or valence band offsets and their influence on electronic and optical properties for AlGaN materials. It is also can be found in Fig. 2 that the energy band gap gradually increases from 1.92 eV to 4.46 eV with the increase of Al content, which is consistent with the experimental results [22]. The increase of energy band gap reduces the efficiency of the electron movement from the valence band to the conduction band since it needs a higher transition energy. On the other hand, compared with GaN, the conduction band bottom offset of $Al_xGa_{1-x}N$ obviously increases from 0.23 eV, 0.53 eV, 0.82 eV, 1 eV to 2.56 eV with x increasing, while the offsets of valence band top are -0.09 eV, -0.06 eV, -0.003 eV, -0.04 eV and 0.03 eV, respectively. It is almost unchanged. From the above analysis, it is can be found that the increase in energy band gap of $Al_xGa_{1-x}N$ is mainly caused by the offset of conduction band bottom, and the changes in electronic and optical properties of $Al_xGa_{1-x}N$ are also mainly affected by the offset of conduction band bottom.

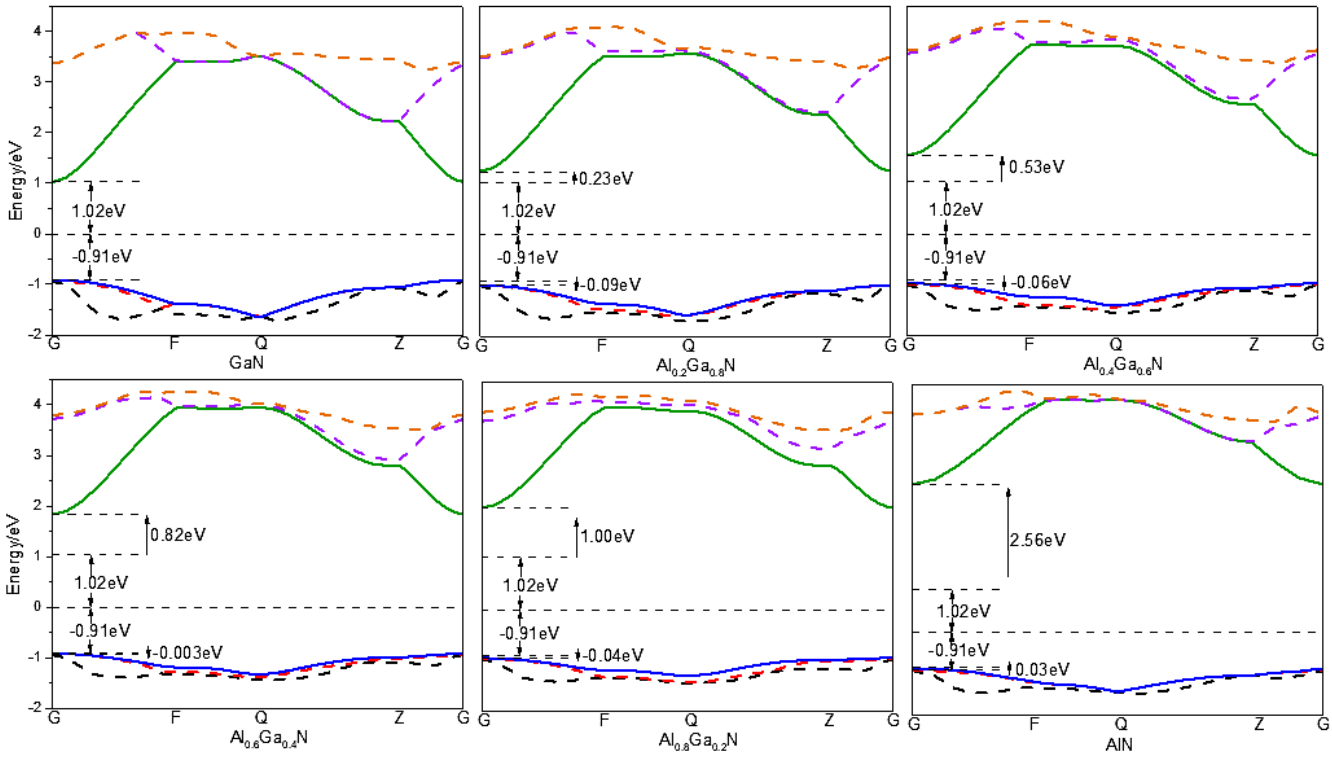

Fig. 2. The energy band structure of wurtzite $Al_xGa_{1-x}N$ (color online)

Contributions of different electronic states in conduction bands and valance bands are responsible for electronic properties of semiconductor material. The influence of various electronic states in conduction bands and valance bands can be obtained from total density of states (TDOS) and partial density of states (PDOS) of semiconductor materials. The TDOS and PDOS of wurtzite $Al_xGa_{1-x}N$ with different Al content are shown in Fig. 3. It can be found that as the Al content increases, the conduction band bottom of $Al_xGa_{1-x}N$ has blue shifts and the energy band gap increases, which is consistent with the results of the energy band structure of wurtzite $Al_xGa_{1-x}N$ as mentioned in Fig. 2. We can also see from Fig. 3 that the TDOS of valence band of $Al_xGa_{1-x}N$ gradually decreases with the increase of Al content from -6 eV to -3.5 eV, which indicates that the total electrons in each orbital decrease. Meanwhile, in the range of -3.5 eV - 0 eV, the TDOS of valance band increases as Al content increases, which means that a large number of electrons collect in valance band top. It improves the probability of electronic transition from valance band to conduction band, and the internal quantum efficiency also increases accordingly, which is beneficial to improving the extraction efficiency of $Al_xGa_{1-x}N$ materials. Another interesting phenomenon is that the TDOS of the conduction band is obviously higher than that of the sum of Al, Ga and N, furthermore, the difference becomes larger with the increase of Al content, which is not reported in previous literature. One possible reason is the lattice structure changes caused by the band shift with the increase of Al content, which can be shown from Fig. 1.

Fig. 3 also shows the PDOS of wurtzite $Al_xGa_{1-x}N$. It can be found that the valence band of GaN mainly consists of N-p, N-d and Ga-s orbitals from -6 eV to -3.5 eV. As Al

content increases, the contributions of Ga-s gradually decrease, the contribution of Al-s orbital gradually increases, where the contributions of N-p and N-d orbitals are almost unchanged. For AlN, the valance band mainly consists of Al-s, N-p and N-d orbitals. In the range of -3.5 eV to 0 eV, Ga-p, Ga-d, N-p and N-d orbitals have major contributions in valance band of GaN. With the increase of Al content, the contributions Ga-p and Ga-d orbitals gradually decrease, the contributions of N-p and N-d orbitals record a slight increase, the contributions of Al-d orbital gradually increase. In the case of x=1, namely, the valance band of AlN mainly consists of Al-d and N-d orbitals. In the range of 0-6 eV, the conduction band of GaN mainly consists of s orbital of Ga and N. with the increase of Al content, the contributions of s orbital of Ga gradually decrease, the contributions of s orbital of N record a slight increase, the contributions of Al-s orbital gradually increase. For AlN, s orbital of Al and N are mainly responsible for electronic contributions in conduction band. From 6 to 9 eV, Ga-s and N-p orbitals are responsible for major electronic contributions in conduction band. As Al content increases, the contributions of Ga-s orbital decrease, the contributions of N-p orbital decrease. For x=0.2, Al-p orbital provides major electronic contributions. For x>0.2, the contributions of Al-p orbital decrease whereas Al-s orbital provide major contributions in conduction band. With the change of electrical properties, the optical properties of $Al_xGa_{1-x}N$, including refractive index, absorption coefficient, and reflectivity coefficient also change accordingly.

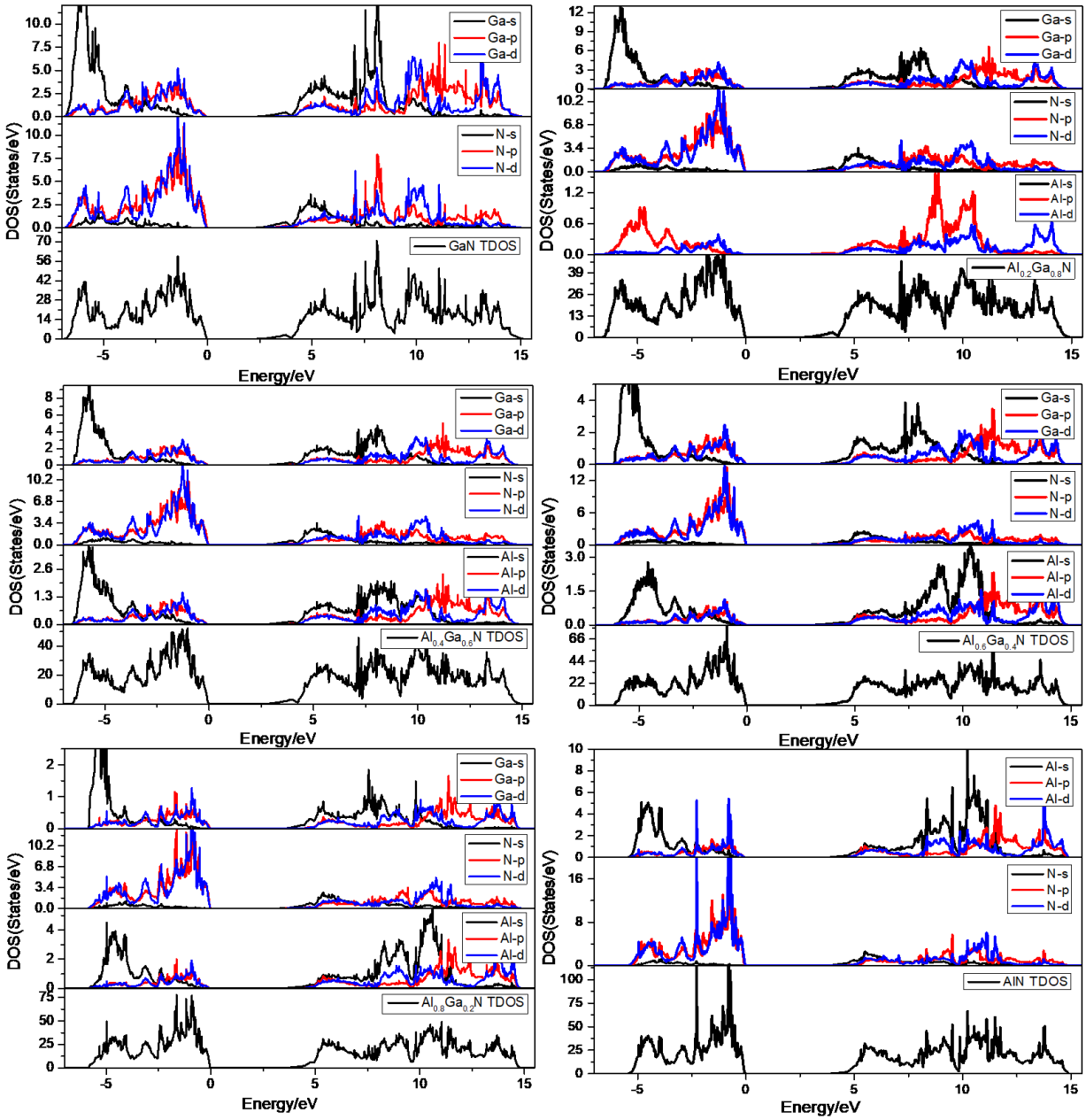

Fig. 3. The total density of states (TDOS) and partial density of states (PDOS) of wurtzite $Al_xGa_{1-x}N$ with different Al content (color online)

3.2. Refractive index

Frequency response of different optical parameters of a semiconductor material to the energy of incident photon ($E=h\gamma$) is explained using optical properties of that semiconductor material. Frequency dependent complex dielectric function $\varepsilon(\omega)=\varepsilon_1(\omega)+i\varepsilon_2(\omega)$ can be used to study different optical parameters of a semiconductor material since it is directly related to energy band structure. Based on the definition of Kramers-Kronig relation and direct transition probability, the real part and imaginary part of the complex dielectric function are calculated from the momentum matrix elements between the wave functions of valence band and conduction band [23].

$$\varepsilon_1(\omega)=1+\frac{2e}{m^2\varepsilon_0}\sum_{\mathrm{v,c}}\int_{BZ}\frac{2dk}{(2\pi)^2}\frac{\left|a\cdot M_{\mathrm{v,c}}(k)\right|}{\frac{\left[E_{\mathrm{c}}(k)-E_{\mathrm{v}}(k)\right]}{h}}\cdot\frac{1}{\frac{[E_{\mathrm{c}}(k)-E_{\mathrm{c}}(k)]^2}{h^2-\omega^2}}, \tag{1}$$

$$\varepsilon_2(\omega)=\frac{\pi}{\varepsilon_0}\left(\frac{e}{m\omega}\right)^2\cdot\sum_{\mathrm{v,c}}\left\{\int_{BZ}\frac{2dk}{(2\pi)^2}\left|a\cdot M_{\mathrm{v,c}}\right|^2\delta\left[E_{\mathrm{c}}(k)-E_{\mathrm{v}}(k)-h\omega\right]\right\}, \tag{2}$$

In which ε_0, h, e and m represent the permittivity of the vacuum, Planck constant, the charge and mass of electron, respectively. $M_{V,C}$ and α represent the transition matrix unit and unit vector of potential A which describes the potential in conduction band or valence band at wave vector k position in the first Brillouin integral zone, respectively. $E_C(k)$, $E_V(k)$ are the intrinsic energy level of the conduction band and valence band at the electron wave vector k, respectively. BZ denotes the first Brillouin integral zone. Thus, after the calculation of complex dielectric function, the complex refractive index, including the real part and imaginary part, can be described as:

$$N(\omega)=n(\omega)+ik(\omega), \tag{3}$$

$$n(\omega)=\frac{1}{\sqrt{2}}\left[\left(\varepsilon_1^2+\varepsilon_2^2\right)^{\frac{1}{2}}+\varepsilon_1\right]^{\frac{1}{2}}, \tag{4}$$

$$k(\omega)=\frac{1}{\sqrt{2}}\left[\left(\varepsilon_1^2+\varepsilon_2^2\right)^{\frac{1}{2}}-\varepsilon_1\right]^{\frac{1}{2}}, \tag{5}$$

where the real part $n(\omega)$ and imaginary part $k(\omega)$ represent the refractive index and extinction coefficient, respectively. Thus, the real part of complex refractive index of $Al_xGa_{1-x}N$ with different Al content x are shown in Fig. 4.

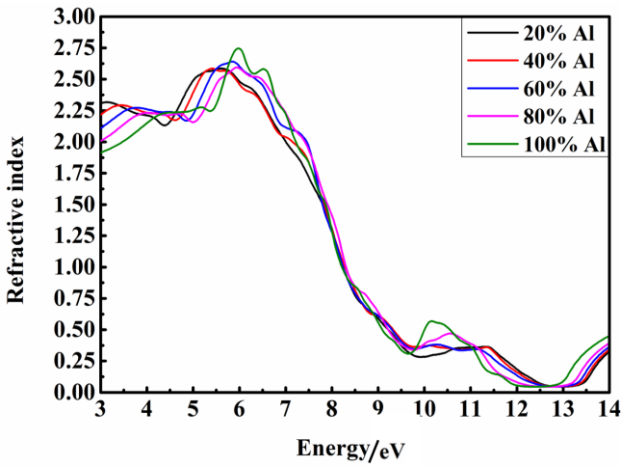

Fig. 4. The calculated refractive index for wurtzite $Al_xGa_{1-x}N$ (color online)

From Fig. 4, it can be found that the refractive index of $Al_xGa_{1-x}N$ decreases as the Al content increases in the range of 0-4.2 eV, where the largest decline occurs from 2.312 to 1.836 at 3 eV. Furthermore, the peak value of the curves decreases with Al content increasing in the range of 3-4.2 eV, which indicate that the refractivity of the material becomes weaker from infrared to 300 nm ultraviolet spectral range, including the whole visible, as the Al content increases. In the range of 5-7 eV and 9.5-12 eV, the peak value of the refractive index increases with the increasing of x, which makes the refraction of the ultraviolet light at the wavelength of 177.5-248.5 nm and 103.5-130.5 nm stronger. The highest peak of the refractive index is 2.75 which is located at 6 eV when x=1. One interesting phenomenon is that the peak value of the reflective index shows a red shift as Al content increases in the range of 9.5-12 eV, which makes the maximum refraction wavelength shift to a longer wavelength. In the range of 12.5-14 eV, with the increase of Al content, the refractive index of $Al_xGa_{1-x}N$ increases which indicates that the refraction of extremely ultraviolet light at the wavelength from 88 nm to 100 nm become stronger.

3.3. Absorption coefficient

The absorption coefficient α describes the intensity attenuation of the light passing through a material. The higher α, the shorter length the light can penetrate into a material which reduce the extraction efficiency for the materials. Absorption coefficient can be defined as the percentage of light intensity attenuation during spreading through unit distance, and can be calculated as [24],

$$\alpha\equiv\frac{2\omega k}{c}=\frac{4\pi k}{\lambda_0}, \tag{6}$$

where c and λ_0 represent the speed and wavelength of light in vacuum, respectively. The absorption coefficient curves of $Al_xGa_{1-x}N$ with different Al content are shown as Fig. 5.

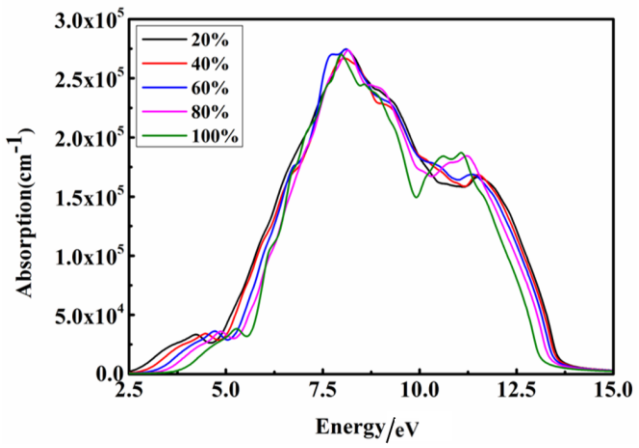

Fig. 5. The calculated absorption coefficient curves of wurtzite $Al_xGa_{1-x}N$ (color online)

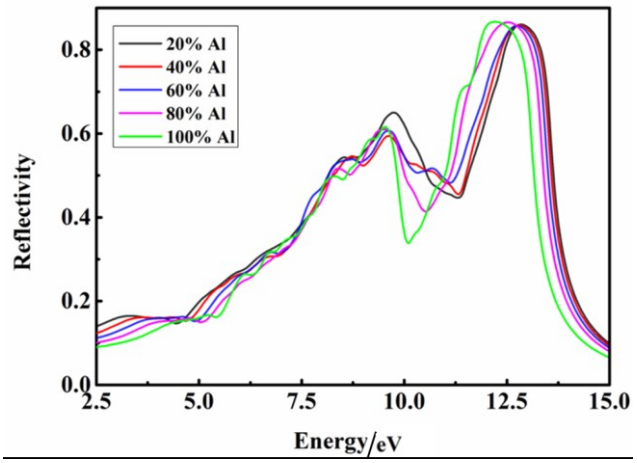

Fig. 6. The calculated reflectivity for wurtzite $Al_xGa_{1-x}N$ (color online)

As shown in Fig. 5, in the range of 2.5-5.75 eV, the absorption of the light decreases with the increase of content of Al content, and the peak value of the absorption coefficient presents blue-shift compared with GaN, which indicate the maximum absorption wavelength of $Al_xGa_{1-x}N$ shift from 293.14 nm to shorter wavelength 235.29 nm. In the range of 7-9 eV, the absorption of $Al_xGa_{1-x}N$ does not show obvious changes as the Al content increases. In the range of 10-12 eV, the absorption of the $Al_xGa_{1-x}N$ material increases with the increase of Al content, in which AlN has the largest absorption coefficient, and obtains a peak value at 11.08 eV. It is beneficial to the light extraction efficiency of the ultraviolet light of the 103.3–124.4 nm wavelength.

3.4. Reflection coefficient

On the basis of reflection law and energy conservation law, the reflection coefficient of wurtzite $Al_xGa_{1-x}N$ can be calculated as

$$R(\omega) = \frac{(n-1)^2 + k^2}{(n+1)^2 + k^2}, \tag{7}$$

where n and k are refractive index and extinction coefficient of materials, respectively. The reflection coefficient curves of wurtzite $Al_xGa_{1-x}N$ with different Al content are shown as Fig. 6.

As shown in Fig. 6, it can be found that the reflectivity of $Al_xGa_{1-x}N$ decreases with increasing Al content in the range of 2.5-5.5 eV. The figure also shows that the peak value does not show obvious changes, while it presents blue-shift to higher energy, which makes the maximum reflection wavelength shift from 375.76 nm to shorter wavelength 236.19 nm. In the range of 7.5-10 eV, the peak value of the reflection curves obtains the maximum reflectivity with 20% Al content at 9.76 eV. It indicates low-Al content $Al_xGa_{1-x}N$ can improve the reflectivity of ultraviolet light at 127.01 nm wavelength. In the range of 11.5-14 eV, the reflectivity increases with increasing Al content, and the peak value shows a red-shift gradually, which makes the maximum reflection wavelength shift to a longer wavelength ultraviolet.

3.5. Energy loss function

The energy loss function, which describes the energy loss of semiconductor when electrons pass through a homogeneous dielectric medium, can be obtained from the complex dielectric function as follows:

$$L(\omega) = \mathrm{Im}\left(\frac{-1}{\varepsilon(\omega)}\right) = \frac{\varepsilon_2(\omega)}{[\varepsilon_1^2(\omega) + \varepsilon_2^2(\omega)]}, \tag{8}$$

where $\varepsilon_1(\omega)$ and $\varepsilon_2(\omega)$ are real part and imaginary part of complex dielectric function. The energy loss curves of wurtzite $Al_xGa_{1-x}N$ with different Al content are shown as Fig. 7.

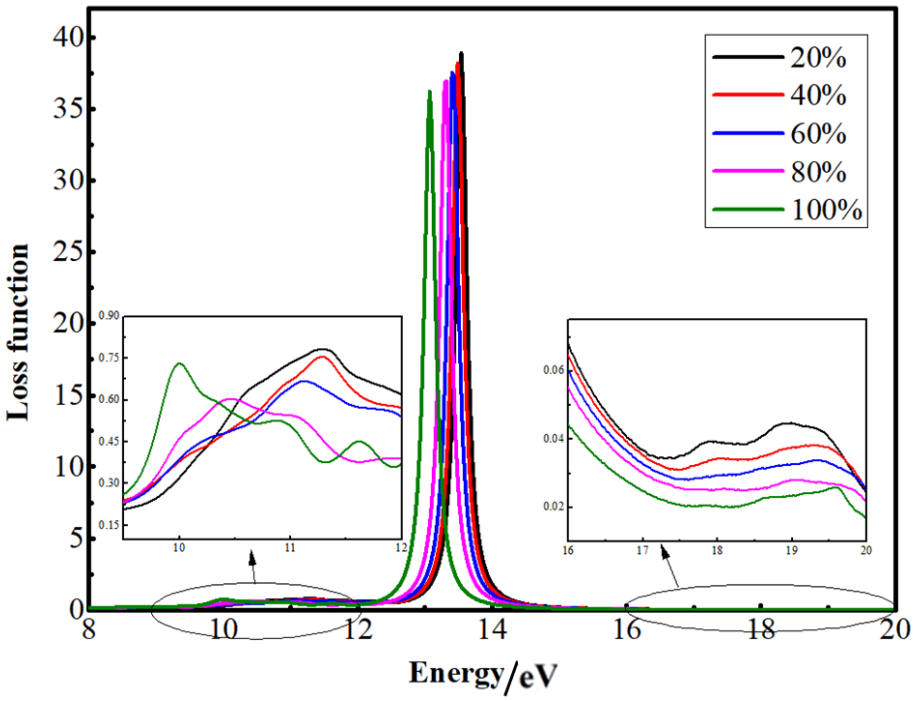

Fig. 7. The calculated energy loss for wurtzite $Al_xGa_{1-x}N$ (color online)

As shown in Fig. 7, as Al content increases, the whole energy loss curves exhibit red shift. In the range of 0-8 eV, the energy loss curves have no obviously changes, which indicates that Al content has little influence on energy loss. In the range of 8-11 eV, as Al content increasing, the energy loss of wurtzite $Al_xGa_{1-x}N$ gradually increases, which reduces the extraction efficiency, and it is unfavorable to produce the ultraviolet from 120 nm to 160 nm spectral range. In the range of 12-14 eV, the energy loss has increases sharply and present a peak value. Furthermore, with the increase of Al content, the peak value of the energy loss decreases gradually and shows red shifted distinctly. In the range of 16-20 eV, the energy loss curves of wurtzite $Al_xGa_{1-x}N$ decreases gradually with the increase of Al content, which is beneficial to the light extraction efficiency of the extremely ultraviolet light of the 62–82 nm wavelength.

4. Conclusion

In this paper, we theoretically calculated the influence of band shift caused by Al content on the opto-electronic properties of $Al_xGa_{1-x}N$ materials based on first-principles. The results show that the Al-doping makes the conduction band bottom of GaN offset, but valence band top is hardly influenced. Along with the increase of Al, the band offset of conduction band bottom increases, which makes the optical properties changed significantly, including refractive index, absorption coefficient and reflection coefficient decrease in the range of 3–6 eV, which is beneficial to the extraction efficiency of ultraviolet light with 206–413 nm. It also provides useful information to design optoelectronic devices based $Al_xGa_{1-x}N$ alloys.

Acknowledgments

This research is Supported by the Joint Opening Project of Anhui Engineering Research Center of Vehicle Display Integrated Systems and Joint Discipline Key Laboratory of Touch Display Materials and Devices in Anhui Province (VDIS2023B03, VDIS&TDMD2024B04, VDIS&TDMD2024D02), the Key Program of Natural Science Foundation of Anhui Provincial Education Department (2023AH050922) and the Excellent Scientific Research and Innovation Teams of Anhui Province (2022AH010059).

References

[1] N. Bouarissa, Mater. Chem. Phys. **73**(1), 51 (2002).
[2] N. Marana, G. Pinhal, J. Laranjeira, P. Buzolin, E. Longo, J. Sambrano, Comput. Mater. Sci. **177**, 109589 (2020).
[3] F. Fichter, Z. Anorg. Chem. **54**(1), 322 (1907).
[4] W. C. Johnson, J. B. Parson, M. C. Crew, J. Phys. Chem. **36**(10), 2651 (1932).
[5] H. M. Manasevit, F. M. Erdmann, W. I. Simpson, J. Electrochem. Soc. **118**(11) 1864 (1971).
[6] H. Amano, N. Sawaki, I. Akasaki, Y. Toyoda, Appl. Phys. Lett. **48**(5), 353 (1986).
[7] H. Amano, M. Kito, K. Hiramatsu I. Akasaki, Jpn. J. Appl. Phys. **28**(12A), 2112 (1989).
[8] D. Brunner, H. Angerer, E. Bustarret, J. Appl. Phys. **82**(10), 5090 (1997).
[9] W. Moseley, A. Allerman, M. H. Crawford, J. Appl. Phys. **117**(9), 095301 (2015).

[10] A. M. Potts, S. Bajaj, D. R. Daughton, A. A. Allerman, A. M. Armstrong, T. Razzak, S. H. Rajan. IEEE Trans. Electron. Devices **68**(9), 4278 (2021).
[11] E. Zielony, R. Szymon, A. Wierzbicka, A. Reszka, M. Sobanska, W. Pervez, Z. R. Zytkiewicz, Appl. Surf. Sci. **588**, 152901 (2022).
[12] M. D. Segall, P. J. Lindan, M. J. Probert, C. J. Pickard, P. J. Hasnip, S. J. Clark, M. C. Payne, J. Phys.: Condens. Matt. **14**(11), 2717 (2002).
[13] V. W. Chris, J. Neugebauer, J. Appl. Phys. **95**(8), 3851 (2004).
[14] C. Stampfl, C. Walle, Appl. Phys. Lett. **72**(4), 459 (1998).
[15] Z. Dridi, B. Bouhafs, P. Ruterana, New J. Phys. **4**, 94 (2002).
[16] L. Lu, Y. Liu, G. Dai, Y. Zhang, G. Ding, Q. Liu, Optik, **164**, 72 (2018).
[17] D. Tang, B. Cao, J. Appl. Phys. **129**(8), 085102 (2021).
[18] M. Yang, B. Chang, M. Wang, Appl. Surf. Sci. **326**, 251 (2015).
[19] J. P. Perdew, K. Burke, M. Ernzerhof, Phys. Rev. Lett. **78**, 3865 (1997).
[20] J. P. Perdew, J. A. Chevary, S. H. Vosko, K. A. Jackson, M. R. Pederson, D. J. Singh, C. Fiolhais, Phys. Rev. B. **46**, 6671 (1992).
[21] P. E. Blochl, Phys. Rev. B **50**, 17953 (1994).
[22] H. Monkhorst, J. Pack, Phys. Rev. B **13**, 5188 (1976).
[23] S. C. Jain, M. Willander, J. Narayan, J. Appl. Phys. **87**(3), 965 (2000).
[24] K. R. Waters, M. S. Hughes, J. Mobley, J. G. Miller, IEEE Trans. Ultrason. Ferr. **50**(1), 68 (2003).

*Corresponding author: daohuawu@ahpu.edu.cn